JOURNAL OF APPLIED ELECTROCHEMISTRY 9 (1979) 255–267

Principles of electrocatalysis and inhibition by electrosorbates and protective layers

J. W. SCHULTZE, M. A. HABIB

Institut für Physikalische Chemie und Quantenchemie, Freie Universität Berlin, Takustrasse 3, Berlin

Received 7 August 1978

Electrocatalysis or inhibition of electrode processes of a reactant R at the metal electrode M is due to the presence of surface layers S. These can be electrostatically adsorbed ions, covalently bound electrosorbates, neutral molecules or layers of oxides and salts, respectively. The influence of layers is caused by electrostatic or chemical interaction between S and R, by a geometric separation of M and R or, in thicker layers, by electronic effects. The influence depends strongly on the type of reaction which can be an outer-sphere electron transfer reaction (ETR), an ion transfer reaction (ITR) or a reaction with formation or breakage of chemical bonds (CBR). Typical examples are discussed for all types of layers and reactions with special emphasis on the type of interaction. Maximum effects are about two orders of magnitude for the electrostatic effect and geometric blocking and about three orders of magnitude for chemical and electronic effects. The theoretical interpretation by changing the pre-exponential factors, activation energies, activity coefficients of the activated complex and transfer coefficients is discussed, but evidence is rare and more detailed experiments are suggested.

1. Introduction

In his investigations of electrocrystallization processes, Hellmuth Fischer did a lot of work on the inhibition of corrosion by organic molecules. Due to his work, various effects of inhibition can be understood [1–8]. Recent progress in all fields of electrosorption theory and thin film phenomena now allows a more general approach to inhibition as well as to catalysis.

The rate of most electrode processes can be changed either by electrode pretreatment or by small additions of a foreign substance which does not participate in the overall electrode reaction. These effects are due to the formation of surface layers of any substance S with partial or complete coverage θ (electrosorbates, $\theta \leqslant 1$) or of thicker layers (protective or passive films with thickness $d > 3$ Å). Models of such surface layers are shown in Figs. 1 and 2 schematically.

The observed current density can change by several orders of magnitude. The effect is called electrocatalysis if i increases, and inhibition if i decreases.

The reason for the catalytic or inhibiting effect may be an electrostatic interaction between the reactant R and the layer S as has been discussed by Frumkin, Parsons *et al.* [9–11, 13–16]. Further, the inhibition by geometric blocking of the surface has been discussed by Fischer [1–8] and many

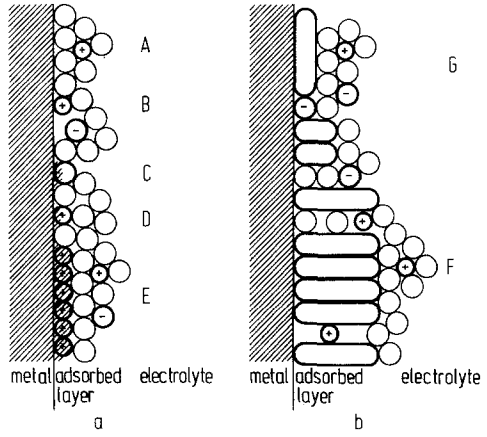

Fig. 1. Schematic representation of double layer model: (a) Ions in the outer Helmholtz layer (A), adsorbed ions in the inner layer without charge transfer (B) and with partial discharge (C, D) and monolayer of completely discharged ions (E); (b) Neutral molecules in perpendicular (F) or parallel orientation (G) as inhibitors of ITR.

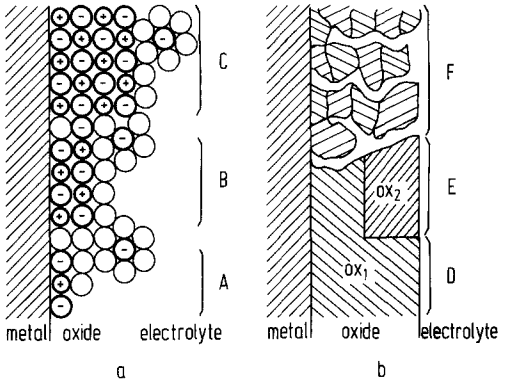

Fig. 2. Schematic oxide layer model: (a) Initial stage of oxide layer formation (A), monolayer (B) and multimolecular layer (C); (b) Homogeneous poreless layer (D), sandwich oxide (E) and porous layer (F).

others [12, 13, 17–22]. More recent experiments have shown that chemical [14, 23–27] and electronic effects [28–30] may also contribute to catalysis and inhibition. Up to now, all these effects have been discussed for special types of layers, reactions or effects, but not in general. Therefore it is the aim of this paper, to demonstrate the influence of these four effects and distinguish between them as far as possible. Since the effects are strongly dependent on the type of layer and the type of reaction, these aspects will be clarified first.

The kinetic influence of surface layers is confined to a small reaction zone (volume) of less than 10 Å but the bulk properties of and the kinetics in the electrolyte e.g. diffusion and homogeneous reactions, are not changed. Hence, the influence of electrosorbed layers can be observed only if bulk effects are not rate determining, i.e. if the current density is smaller than the limiting current controlled by diffusion or reaction.

2. Experimental data

In an electrode reaction, a reactant R^{z_R} forms a product P^{z_R+n} according to

$$R^{z_R} \rightarrow P^{z_R+n} + ne^- \qquad (1)$$

where z_R is the charge of the reactant and n the number of electrons exchanged with the metal electrode M. The current density i of Reaction 1 can be measured by considering its dependence on the variables

$$i = f(c_R, c_X, T, \eta, \theta) \qquad (2)$$

where c_R = concentration of R, c_X = concentration of foreign substances, e.g. excess electrolyte, pH or others, T = temperature, η = overvoltage and θ = coverage or thickness of layer S. For anodic reactions, equations of the type

$$\ln i = \ln k_m c_R nF + g(\theta) - \frac{\Delta H^{\ddagger}}{RT} + \frac{\alpha nF\eta}{RT} \qquad (3)$$

are expected, where k_m = maximum rate constant, $g(\theta)$ = any function of θ, $\Delta H^{\ddagger}$ = activation enthalpy at the equilibrium potential and α = anodic transfer coefficient. The electrochemical reaction order [31] $\nu_R = 1$ is taken for simplicity in Equations 1 and 3 as well. In the case of cathodic reactions, the last term in Equation 3 must be replaced by $-(1-\alpha)nF\eta/RT$. Most experimental results are less distinctive than Equation 3. Many experiments are carried out at the equilibrium potential only, yielding the standard rate constant

$$k(\theta) = i_0/c_R nF \qquad (4)$$

which depends on the coverage θ. Various experiments have been carried out with dependence on the overvoltage, but very few experiments refer to the temperature dependence of i [30]. Hence, the separation of the influence of S on k, or $\Delta H^{\ddagger}$ is possible for few systems only, but usually the mixed effects are observed.

Many results refer to multi-step reactions. Here another difficulty arises. If intermediates are formed, it is difficult to see if hindered steps are catalysed or if poisoning of the electrode is inhibited, e.g. the oxidation of HCOOH on Pt in the presence of electrosorbed metal ions [24].

Finally, different effects can cause similar changes of kinetic data. For example, the activation enthalpy can be changed by chemical effects, by a change in the geometry of the reacting system [32] or by a contribution of the electronic effects [30]. For all these reasons, the interpretation of experimental data is sometimes speculative and more experimental work is necessary to give evidence for special effects. In spite of these limitations, some general features can be shown in the following discussion.

3. Types of reactions

The influence of layers on the rate of electrode processes depends very much on the elementary act which is rate determining. The following reactions can be distinguished.

3.1. *Outer-sphere electron transfer reactions (ETR)*

After rearrangement of the solvent, the ETR takes place at a constant electronic energy. Since the hydration shell of R is unchanged during the reaction, the process must take place from the outer Helmholtz layer or even from larger distances from the metal. Some examples are Eu^{3+}/Eu^{2+}, Fe^{3+}/Fe^{2+} or $[Fe(CN)_6]^{4-}/[Fe(CN)_6]^{3-}$ [19, 20, 28, 41, 42]. The ETR can be explained in terms of the Marcus theory [33–38] or of the Gurney–Gerischer theory [39, 40]. An influence of S can be expected if the electronic interaction between M and R or the concentration of R is influenced by a change of the potential distribution in the double layer.

3.2. *Ion transfer reactions (ITR)*

In this case, the ions must be transferred through the double layer from the electrode to the surface and vice versa. This process follows the classical Butler–Volmer mechanism [31]. The activated complex is expected to be in the inner layer. Strong electrostatic or chemical influence or geometric blocking may be expected. Metal deposition or dissolution reactions such as Zn^{2+}/Zn [22], Cd^{2+}/Cd [21], etc., fall into this category of reactions. Transfer reactions of anions e.g. OH^- and Cl^- occur at the surface of oxides and halides, respectively.

3.3. *Redox reactions involving the formation or breakage of chemical bonds (CBR)*

The ETR or ITR may be followed or preceded by the formation or breakage of chemical bonds. Most multistep reactions fall into this category, e.g. the evolution of hydrogen and oxygen or the oxidation of CO to CO_2. In these cases electrosorbed intermediates are formed mostly. Hence, chemical or electrostatic interactions are most probable, but geometric blocking is possible too. Energetic aspects of multistep reactions on nonmetallic surfaces were discussed by Gerischer [103].

4. Types of layers

To estimate the influence of the catalyzing or inhibiting species, the coverage, the geometry and the charge of S must be known. The coverage can be determined by the methods of analytical chemistry or by means of thermodynamics. The geometry can be estimated from comparing capacity data with ionic radii and molecular models, respectively. The charge of electrosorbed substances can be estimated from the electrosorption valency [43]. There are some limiting cases which can be used for the classification of layers. Real systems, of course, can show an intermediate behaviour. In Figs. 1 and 2, double layer structures with different types of layers are shown.

4.1. *Ionic adsorbed layers*

These layers are formed by electrosorption of ions from the solution without charge transfer (Fig. 1a, case B). Because of the electrostatic repulsion between the adsorbed ions, the coverage of them is generally small, i.e. less than 30%. Chloride ions adsorbed on Hg are a typical example [44]. Bromide and iodide ions are taken for ionic adsorbates too [15, 16, 42, 45] but there is a significant discharge of these ions at mercury (Fig. 1a, case C) and an almost complete discharge at gold electrodes. Discharge of ions and formation of covalent bonds both increase with decreasing difference of Paulings electronegativities $\Delta\chi = |\chi_M - \chi_S|$ [43, 46]. This becomes important for $\Delta\chi < 1$. The most important effect of ionic layers is due to electrostatic and chemical interactions with R. Geometric and electronic effects are small since $\theta < 0{\cdot}3$.

4.2 *Covalent adsorbed layers*

Formation of these layers takes place when the electrosorbed ions are completely discharged $\Delta\chi < 0{\cdot}4$ [43]. Since the electrostatic repulsion between the ions decreases with decreasing charge, monolayers of these covalently adsorbed ions

(Fig. 1a, case E) are formed easily [43]. The double layers and the adsorbed water molecules are shifted to the electrolyte side. Well-known examples are the metallic monolayers [23, 24] and sulphide layers [25, 26, 104]. Only chemical effects are expected for these layers and the electrostatic influence is negligible. If the surface of the metal M is active and S is inactive, the influence of the covalent layers will be a geometric blocking or poisoning.

4.3. *Layers of neutral molecules*

Neutral molecules including polymers (Fig. 1b) are used as inhibitors in many systems [12, 13, 17–21, 47, 48]. The most important influence of these layers is the geometric blocking. In general, the chemical and electrostatic influence with the reactant is small. Exact calculations take the Frumkin effect into account [20].

4.4. *Oxide layers*

These layers can be formed by anodic polarization of the metal electrodes. The thickness, d, of the layers depends on the potential and the time of polarization [49]. Since these layers are semiconductors or insulators, tunnelling of electrons from R to the bands of the oxide and metal, respectively, is expected and electronic effects are important [28, 29, 50]. For thin layers or small coverages, blocking can be expected [51, 102]. Chemical interactions between the oxide layer and R can be expected for CBR. Various types of layers can be distinguished with reference to their structure. Film growth according to a field-dependent ion transport mechanism yields tight passive films (Fig. 2b, case D). If nucleation is important, they can grow by an island mechanism. Anodic deposition from the solution, on the other hand, yields porous layers (Fig. 2b, case F). Combinations of various types, multiple layers (sandwich-type; Fig. 2b, case E) may also occur.

4.5. *Salt layers*

Salt layers are very similar to oxide layers, and can be tight, porous or islands (Fig. 2b). The formation takes place during the anodic dissolution of metals as well as by precipitation from the electrolyte. Chemical, geometric and electronic effects are expected in such a case. Typical examples are the layers of $NiCl_2$ formed during the anodic dissolution of nickel [53] and the passivating layers of LiCl formed on lithium electrodes in $SOCl_2$ solution [54].

5. Influence of electrostatic interactions

We define the Coulombic attraction or repulsion between the reactant, R, and the adsorbed layer, S, as electrostatic interaction. These interactions can always be expected if the charges z_S and z_R differ from zero. Hence they will be important for ionic layers but negligible for all others, where ions are discharged or their charge is compensated by counterions. Electrostatic attraction ($z_S z_R < 0$) yields catalysis, and repulsion ($z_S z_R > 0$) yields inhibition. The rate changes caused by electrostatic interaction can be up to three orders of magnitude. Interactions between ions and dipoles are of less importance. These secondary effects will not be discussed here.

5.1. *The Frumkin effect*

The so-called Frumkin effect [9] takes into account the change of c_R in the outer Helmholtz plane (OHP) due to the diffuse layer potential ψ_d. Further, the rate-determining potential drop in the Helmholtz layer is not given by η but by $(\eta - \psi_d)$ [101]. For the anodic case, we have

$$i = kc_R \exp\left(-\frac{z_R F \psi_d}{RT}\right) \exp\left[\frac{\alpha n F(\eta - \psi_d)}{RT}\right]. \tag{5}$$

Since $(d\psi_d/d\theta) \sim z_S$, the Frumkin effect can be described by the derivatives

$$\frac{d \ln i}{d\psi_d} = -\frac{F}{RT}(z_R + \alpha n)$$

and

$$\frac{d \ln i}{d\theta} \sim \frac{-z_S z_R}{RT}\left(1 + \frac{\alpha n}{z_R}\right). \tag{6}$$

The potential ψ_d can reach 50 mV or more. Therefore, the Frumkin effect can cause changes of i by one or more orders of magnitude. In the case of outer-sphere ETR, the Frumkin effect explains quantitatively the influence of S on the current density, e.g. in the case of Eu^{2+}/Eu^{3+} [41] or

Table 1. Maximum electrostatic influence of halide ions adsorbed at mercury on electrode processes. (Data were corrected for Frumkin effect).

Reaction	*Layer*	θ	$\Delta \log k$	*Types of reaction*	*Reference*
Eu^{2+}/Eu^{3+}	Cl^-, I^-	< 0·3	0	ETR	41
H^+/H_2	Cl^-, I^-	< 0·1	+ 2	CBR	10, 97
Zn^{2+}/Zn	Br^-, I^-	< 0·06	+ 1·2	ITR	45
BrO_4^-	Cl^-, Br^-	< 0·3	− 1	CBR	16
$S_4O_6^{2-}$	Br^-, I^-	< 0·3	− 1·7	CBR	58, 59

Cr^{2+}/Cr^{3+} [55], but in the case of ITR or CBR, additional effects occur.

In the following sections, we will neglect the Frumkin effect to simplify the discussions. Experimentally, this can be justified using higher concentrations of the supporting electrolyte.

5.2. *Electrostatic influence on the activated complex*

In the case of ITR and CBR, the activated complex is formed in the inner layer, where the electrostatic influence of adsorbed ions is even stronger. Typical examples are the cathodic hydrogen evolution or metal deposition on mercury, which are catalysed by adsorbed halide ions (Fig. 1a, case B) or the cathodic reduction of bromate ions which is inhibited [14]. Some experimental data are collected in Figs. 3 and 4 and maximum effects for some cases are shown in Table 1.

5.2.1. Parson's theory. Parsons [10, 11] gave an interesting explanation of the electrostatic effect. He took into account the change of the activity coefficient $a^{\ddagger}$ of the activated complex which should be influenced by the electrostatic interaction with the adsorbed ions, which are treated as two-dimensional gas. $a^{\ddagger}$ may be written as dependent on the ionic coverage

$$a^{\ddagger} = N_m(1-\theta)^{-1} \exp(2B_{\ddagger,S}\theta) \qquad (7)$$

where N_m is the total number of sites in the interphase and $B_{\ddagger,S}$ is the second virial coefficient* due to the interactions between the ion S and the activated complex. In Equation 7, $p = 1$ was assumed for the ratio of the area occupied by the complex to that occupied by a solvent molecule; for the general case see [10]. In the case of strong interactions and small coverages, the pre-exponential term is almost constant. Since the rate constant is proportional to $1/a^{\ddagger}$, the influence of adsorbed ions can be approximated by

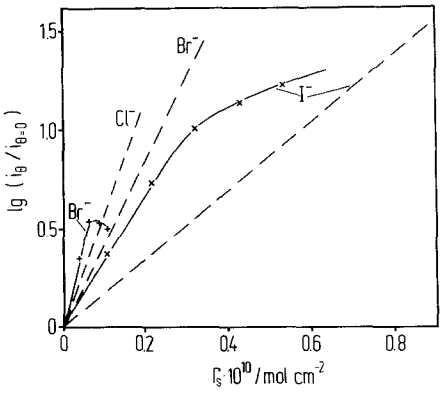

Fig. 3. Electrostatic influence on the cathodic reduction of $2H^+ + 2e^- \rightarrow H_2$ (- - - - -) [10] and $Zn^{2+} + 2e^- \rightarrow Zn$ (———) [45] on mercury by the adsorbed ions.

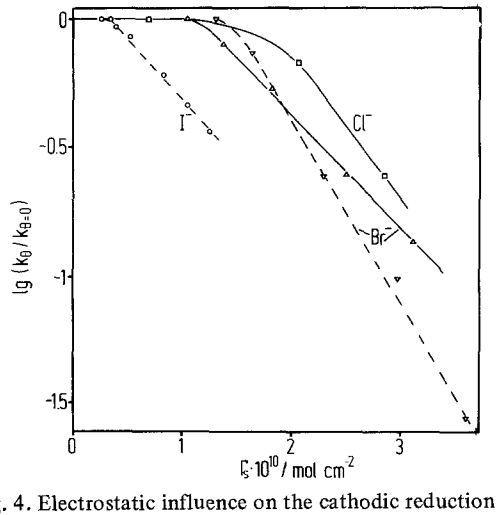

Fig. 4. Electrostatic influence on the cathodic reduction of BrO_4^- (———) [16] and $S_4O_6^{2-}$ (- - - -) [58] ions on mercury by the electrosorbed ions.

* The second virial coefficient $B_{\ddagger,S}$ may be related to the virial coefficient $B_{S,S}$ which expresses the first order interaction between the adsorbed ions themselves, by $B_{\ddagger,S} = (z_{\ddagger}/z_S)B_{S,S}$.

Table 2. The slopes of $\Delta \log i - \Gamma_S$ *plots of Figs. 3 and 4 indicating the electrostatic interaction*

	$d(\Delta \log i)/d\Gamma_S \times 10^{-10}$ cm^2 mol^{-1}		
Electrode reaction	Cl^-	Br^-	I^-
H^+/H_2	5·587	4·219	1·736
Zn^{2+}/Zn	–	13·699	3·114
BrO_4^- reduction	−0·567	− 0·469	–
$S_4O_6^{2-}$ reduction	–	− 0·714	0·470

$$\Delta \ln i = \ln (i/i_{\theta=0}) = \ln (k/k_{\theta=0}) = -2B_{\ddagger,S}\theta. \quad (8)$$

According to Equation 8, a plot of the logarithm of the rate at constant potential against the amount of adsorbed ions would be expected to be linear. In fact, this was observed for cathodic hydrogen evolution on Hg by Parsons [10], for the $Zn^{2+}/Zn(Hg)$ reaction by Sluyters *et al.* [45, 56] and for the $Ni^{2+}/Ni(Hg)$ reaction by Eriksrud [57]. Some examples are shown in Fig. 3. Equation 8 is valid up to $q_i = 10\,\mu C\,cm^{-2}$, i.e. 0·1. At higher coverages, however, the slope of the lines decreases indicating inhibiting effects by the increasing ionic population in the double layer. Fig. 4 shows the same plot for the reduction of BrO_4^- and $S_4O_6^{2-}$ ions on mercury observed by Guidelli *et al.* [16, 58, 59], which shows a similar behaviour for the case of inhibition.

The slopes of the lines in Figs. 3 and 4 should be proportional to the Coulombic interaction between R and S, which is proportional to $z_\ddagger z_S$. Hence, reactions of cations and anions are catalysed and inhibited respectively by adsorbed halide ions. This is confirmed by Figs. 3 and 4. On the other hand, the electrostatic effect of Cl^- should be the same as that of Br^- and I^- at the same value of Γ_S. This is not confirmed by experiment (Table 2). In all cases, the influence decreases in the sequence $Cl^- > Br^- > I^-$. This effect is due to the partial discharge of the halides which increases from Cl^- to I^- due to the decreasing electronegativity χ [43]. The empirical correlation between the electrosorption valency γ and $\Delta\chi$ suggests an effective charge of $1e$ for adsorbed Cl^-, but about $0{\cdot}6e$ or less for the adsorbed I^-. The observed decrease of the electrostatic influence of these ions supports the assumption of an increasing discharge of Br^- and I^-.

5.2.2. Guidelli's theory. Guidelli and co-workers [15, 16, 58–60] treated the electrostatic interaction between R and S in another way, based more on an electrostatic double layer model and starting from Hush's theory of electrode kinetics [63] and neglecting any partial discharge of adsorbed anions. They express the influence of adsorbed ions by

$$\ln \frac{k}{k_{\theta=0}} = \begin{cases} -\dfrac{(z_R - \alpha)F}{RT}\,\dfrac{4\pi q_S x_i}{D}\left(1 - \dfrac{x_\ddagger}{x_0}\right) \\ \text{for} \quad x_\ddagger \geqslant x_i \qquad (9) \\ -\dfrac{(z_R - \alpha)F}{RT}\,\dfrac{4\pi q_S x_\ddagger}{D}\left(1 - \dfrac{x_i}{x_0}\right) \\ \text{for} \quad x_\ddagger \leqslant x_i \qquad (10) \end{cases}$$

where x_i and x_0 denote the distances of the inner and outer Helmholtz plane, respectively, from the electrode surface ($x = 0$) and D is the dielectric constant for the compact layer. Using the respective ionic radii $r_i = x_i$, Equation 9 predicts $\Delta \ln k_{Cl^-}/\Delta \ln k_{I^-} = r_{Cl^-}/r_{I^-} = 1{\cdot}8/2{\cdot}2 < 1$ in clear contradiction to the experiments. Equation 10, on the other hand, predicts the correct sequence $\Delta \ln k_{Cl^-} > \Delta \ln k_{I^-}$. If this electrostatic model is to be valid, however, the electrosorption valency γ of Cl^- should exceed that of I^-, but the contrary is observed, $|\gamma_{Cl^-}| = 0{\cdot}2 < |\gamma_{I^-}| = 0{\cdot}45$, since the partial discharge is negligible for Cl^- but not for I^- [61]. Hence, the pure electrostatic assumptions of the Guidelli model are in conflict with experimental data, and Equations 9 and 10 cannot be used without corrections.

Taking into account the partial charge transfer, $q_S = z_S\Gamma_S$ [83–89] where z_S is the effective charge on the adsorbed ion S, Equations 9 and 10 yield the correct sequence $\Delta \ln k_{Cl^-} > \Delta \ln k_{I^-}$,

since the changes in z_S exceed those of x_i.

Guidelli's and Parsons' theories both predict the linear shape of $\ln i/\Gamma_S$ plots. Both theories are insufficient, if the partial charge transfer is neglected. The inclusion of partial charge transfer gives qualitatively correct predictions, but not quantitative agreement.

As Guidelli *et al.* [64] have shown, there is no basic difference between Parsons' approach and that of Guidelli. Later Guidelli *et al.* [64] included the consideration of diffuse layer potential into their theory which, however, did not change the predictions of the theory significantly. Thus, the main difference between these two theories is the inclusion of ψ_d in Guidelli's theory and its neglect in Parsons' approach.

Levine and Fawcett [65] also put forward a theory on the basis of the discreteness of charge effect, to account for the influence of electrosorbates on electrode processes. This theory [65] has been shown also to be basically same as that of Guidelli [64] *.

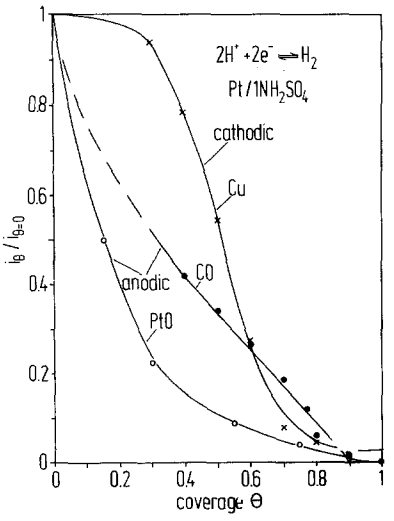

Fig. 5. Geometric blocking of the reaction $2H^+ + 2e^- \rightarrow H_2$ on Pt in 1 N H_2SO_4 by Cu [71], CO [100] and PtO [102].

6. Geometric blocking effect

Physical separation of M and R by an adsorbed substance can cause a decrease of the reaction rate by various orders of magnitude for all types of reactions. The inhibition of ETR and ITR by adsorbed large organic molecules has been discussed extensively by Fischer [1–8] and many others [12, 13, 17–22]. In the case of ITR and CBR, however, even small inorganic molecules, atoms or ions can cause inhibition. For example, the anodic dissolution of iron is inhibited with the increasing coverage of ferrous oxide on the iron surface [51]. Further examples are summarized in Table 3. Fig. 5 shows the geometric blocking of the anodic or cathodic reaction

$$H_2 \rightleftharpoons 2H^+ + 2e^-$$

on platinum caused by an increasing coverage of oxide, CO and Cu, respectively. For all these reactions, a continuous decrease of i down to $i \approx 0$ at $\theta = 1$ is typical.

Due to the separation of M and R, the reaction rate is zero or very small for a complete monolayer of S. For intermediate coverages, a decrease with $(1-\theta)$ can be expected, but this is observed only in very simple systems. In general, two types of inhibition must be distinguished. On homogeneous surfaces, inhibition must be due to changes in the double layer structure. On heterogeneous solid surfaces, however, the different coverage on different crystal planes can be very important.

Table 3. Maximum effect of geometric blocking

Reaction	*Electrode*	*Adsorbed layer*	θ	$\Delta \log k$	*Types of reaction*	*Reference*
$[Fe(CN)_6]^{4-}/[Fe(CN)_6]^{3-}$	Hg	n-$C_5H_{11}OH$	≈ 1	−1·5	ETR	19, 20
H^+/H_2 (anod.)	Pt	CO	≈ 1	−2·0	CBR	100
H^+/H_2 (cath.)	Pt	Cu	< 1	−1·5	CBR	71
H^+/H_2 (anod.)	Pt	PtO	≈ 1	−2·0	CBR	102
Zn^{2+}/Zn	Hg	$C_6H_{13}OH$	≈ 1	−2·0	ITR	22
Cd^{2+}/Cd	Hg	$C_5H_{11}COOH$	≈ 1	−2·5	ITR	21
Fe^{3+}/Fe	Fe	Fe_2O_3	> 1 ($d \approx 30$ Å)	−4·0	ITR	31

* For a detailed comparison, see [64].

6.1. *Geometric blocking on homogeneous surfaces*

Early inhibition studies started with the inhibition of ITR on mercury [9, 12]. Parsons [11] attributed the changes of rate constant to the interactions of the activated complex with surrounding adsorbed molecules, yielding an expression of the type

$$\Delta \ln i = \Delta \ln k = -2B_{\ddagger,S}\theta + p \ln (1-\theta) \tag{11}$$

which is very similar to Equation 8. The interaction parameter was also the basic idea of Kastening's [13] approach but he included it in the activation enthalpy. Laitinen and Biegler [17] argued that the basic effect is the geometric separation of M and R yielding an increase of activation energy

$$\ln \frac{k}{k_{\theta=0}} = -\left(\frac{H_{\theta=1} - H_\theta}{RT}\right) = \theta \ln (k_{\theta=1}/k_{\theta=0}). \tag{12}$$

The same idea was used later by Jaenicke and Schweitzer [32] for the explanation of the influence of the solvent composition on ITR. The temperature dependence was proved by Loshkarev *et al.* [21]. They showed that k_m increases, and α remains constant or decreases with rise of temperature. For some systems $B_{\ddagger,S}$ is negligible, and Equation 11 reduces to the simple dependence $k\alpha(1-\theta)$, which was found by Sathyanarayana for the inhibition of the deposition of Cu^{2+}, Cd^{2+} and Zn^{2-} on Hg by *n*-butanol [66]. The inhibition of oxygen reduction on Hg by *n*-butanol also follows such an equation showing the blocking effect [11].

However, not all organic compounds inhibit electrode reactions. Especially those organic compounds adsorbed as radicals can react with R causing a catalysis (see Section 7).

Special effects are observed with ETR on metal electrodes covered with inhibitors. Then, the transfer coefficient can also change [67] due to a decreasing overlap between M and R which will be discussed in Section 8 (electronic effects).

6.2. *Geometric blocking on heterogeneous surfaces*

The surfaces of solid metals consist of various crystal planes, e.g. platinum or gold surfaces are composed, in part, of (1 1 1), (1 0 0) and (1 1 0) planes [68, 69]. Rate constants of ETR will be independent of the crystal orientation, but the rate of ITR and CBR can strongly depend on the plane. Hence, not only one constant $k_{\theta=0}$ exists, but a sum of constants $\Sigma\, k_{j,\theta=0}$ must be considered for all crystal planes. The adsorption enthalpy of S differs on various planes, e.g. for f c c metals, it decreases mostly in the sequence (1 1 0) > (1 0 0) > (1 1 1) [70]. If the adsorption of the reactant R follows the same sequence, i will decrease with $(1-\theta)$ or very similar to that (see Fig. 5). If R reacts preferably on another plane, e.g. (1 1 1), a small coverage of S, $\theta < 0{\cdot}5$, which refers to another plane, will have no influence. This seems to be the case for the inhibition of the cathodic hydrogen evolution on Pt by Cu [71] shown in Fig. 5 where i decreases for $\theta_{Cu} > 0{\cdot}3$ only. For the hydrogen oxidation, further complications arise from the condition that two neighbouring adsorption places must be available, which yields an expression containing a $(1-\theta)^2$ term. Summarizing these effects, a generalized equation must be used instead of Equation 11:

$$i = \sum i_j = c_R nF \sum_j \left\{ \frac{k_{j,m}(1-\theta_j)}{a_{\ddagger,j}} \times \exp\left[-\frac{\Delta H^{\ddagger}(\theta) - \alpha nF\eta}{RT}\right]\right\} \tag{13}$$

which can be transformed for very simple systems to Equation 11 or the simple $(1-\theta)$ dependence.

7. Chemical interactions

If a chemical bond is formed between S and R, a new intermediate is formed in the electrode reactions. Then, the reaction mechanism changes as well as the reaction rate. The formal description of chemical interactions must take into account the coverage of S–R which should be proportional to θ, the activation energy $\Delta H^{\ddagger}$ and the transfer coefficient α. The total rate is the sum of the rate on the free surface and that of the catalysed reaction and can be obtained by analogy to Equation 13, where the constant $k_{j,m}$ should now include a formation constant $k_{R\text{-}S}$ of the new intermediate.

Of course, the formation of an intermediate S–R can cause a decrease in rate, which could be called a poisoning. Experimentally, however, this

Table 4. Maximum effect of chemical influence of layers on CBR (Data for SCN^- are corrected for the Frumkin effect.)

Reaction	*Electrode*	*Layer*	θ	$\Delta \log k$	*Reference*
CO/CO_2	Pt	PtO	< 1	$+ 3$	27
$HCOOH/CO_2$	Pt	S	0·4	$+ 1$	25
O_2/H_2O	Au	Bi^{3+}	≈ 1	$+ 1{\cdot}5$	23
In^{3+}/In	Hg	SCN^-	$< 0{\cdot}5$	$+ 1{\cdot}3$	75, 76
Eu^{3+}/Eu^{2+}	Hg	SCN^-	$< 0{\cdot}5$	$+ 1$	74
Cr^{3+}/Cr^{2+}	Hg	SCN^-	$< 0{\cdot}5$	$+ 1$	74

poisoning is very similar to inhibition by geometric blocking of the surface and will not be discussed here.

The catalysis by chemical interaction, on the other hand, differs from geometric effects, because it can be observed even at very low coverages of S. If the rate constant increases by several orders of magnitude, the product $k\theta$ can exceed the reaction rate at the free surface $k_{\theta=0}(1-\theta)$ even at small coverages $\theta = 0{\cdot}1$ or less. Chemical interactions are short ranged, they refer to distances of less than 2 Å. Hence, they are important in the Helmholtz layer, i.e. for ITR and CBR. In the case of ETR, chemical interactions are excluded by definition. Experimentally, this was verified by Adzic and Despic [72]. Some typical examples are summarized in Table 4. The anodic oxidation of CO on platinum is catalysed by oxide (see Fig. 6, curve a [27]) or sulphide layers [25, 26]. In a similar way, the oxidation of HCOOH is catalysed by sulphide layers. As has been shown by Sandstede *et al.*, the activation enthalpy decreases by about 30 kJ mol^{-1} [26]. At gold electrodes, the reduction of oxygen is catalysed by a monolayer of Bi [23]. Metallic monolayers (Cd^{2+}, Pb^{2+}, Tl^+, Bi^{3+}) are also found to catalyse the oxidation of HCOOH on Pt, but it is suggested that this catalysis is in fact an inhibition of poisoning by the adsorption of a COH species [24]. The adsorbed metal ions inhibit the hydrogen adsorption (see Fig. 5). Since the poisoning species will be adsorbed probably also via the hydrogen atom, the surface is blocked for this species but not for further oxidation of HCOOH, which can take place easily on the metallic conducting electrosorbate.

The catalysis of the hydrogen evolution reaction on Hg in the presence of electrosorbed N-heterocyclic compounds is due to the neutralizing properties of the radical RNH^+_{ads} formed in a prior chemical recombination step

$$RN_{sol} + H^+ \rightarrow RNH^+_{ads} \text{ [73]}.$$

The change of mechanism can be demonstrated with ETR, e.g. the reduction of Eu^{3+} or Cr^{3+}. In the presence of SCN^- which is strongly adsorbed on Hg, the reaction mechanism changes to an inner-sphere electron transfer reaction which is much faster than the ETR [74]. The catalysis of an ITR by chemical interaction can be demonstrated by the reduction of indium

$$In^{3+} + 3e^- \rightarrow In(Hg)$$

which is catalysed again by SCN^- [75, 76]. These ions form with In^{3+} an adsorbed complex $In(SCN)^+_{2,ads}$ which releases, after reduction, the two SCN^- ions. In this way, the direct ITR is substituted by CBR.

In all cases of catalysis by ions, however, the electrostatic influence is very important, too.

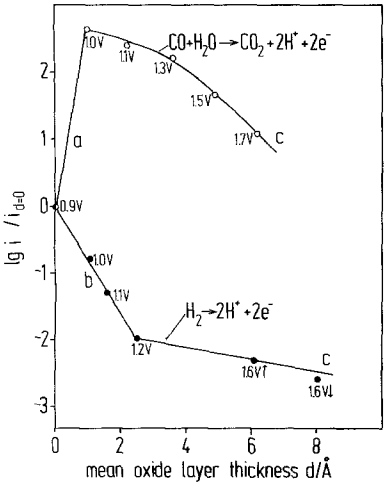

Fig. 6. Influence of d_{PtO} on anodic reactions at Pt: (a) Catalysis of $H_2O + CO \rightarrow CO_2 + 2H^+ + 2e^-$; (b) geometric blocking of $H_2 \rightarrow 2H^+ + 2e^-$; and (c) electronic influence on both reactions. Data are taken from [27] and [102]; for details see [29].

Table 5. Maximum electronic influence of oxide layer on ETR and CBR

Reactions	*Electrode*	*Layer*	*d* (Å)	*Effect*	$\Delta \log k$	*Types of reaction*	*Reference*
H_2O/O_2	Pt	PtO	7	tunnelling ($\epsilon < 1{\cdot}8$ V)	-4	CBR	29
H_2O/O_2	Pt	PtO	7	resonance tunnelling ($\epsilon > 1{\cdot}8$ V)	$+1$	CBR	30
$[Fe(CN)_6]^{4-}/[Fe(CN)_6]^{3-}$	Fe	Fe_2O_3	30	tunnelling (cond. band)	$-1{\cdot}5$	ETR	78
Fe^{2+}/Fe^{3+}	Ti	TiO_2	50	resonance tunnelling	$+3$	ETR	81

Special attention must be paid to the elimination of these effects.

8. Electronic effects

In the case of semiconducting layers on electrodes, the rate of a reaction can change in spite of constant chemical surface composition, complete geometric blocking of the metal surface and negligible electrostatic effects (Table 5). Then, the electronic structure of the surface layer may be important and causes changes of the reaction rate of inner- or outer-sphere electron transfer reactions by various orders of magnitude. The electronic structure of a surface layer depends on its thickness [49], the band gap and the concentration of donors and acceptors, respectively [77]. In the case of monomolecular layers, only localized electron terms exist in the oxide which do not participate in electron transfer. Hence, the electron must tunnel from R to M and vice versa. The electron transfer takes place mostly at the Fermi level. Then, the activation energy of the reaction does not change, but the pre-exponential factor decreases exponentially with increasing thickness. Experimentally, the relation

$$\log(i/i_{d=0}) = -d/d_0 ; \log(k_m/k_{d=0}) = -d/d_0 \quad (14)$$

was found at constant potential with d_0 and $i_{d=0}$ constants [28–30]. Examples are shown in Fig. 7 for ETR as well as CBR on oxide covered platinum. At thicker layers, the bands of the layer and impurity terms, e.g. donors, participate in the electron transfer. The participation of lower or higher electron terms of the oxide causes an increase of the activation energy. The pre-exponential factor depends strongly on the band structure and the tunnel distance [30, 78, 79]. At passivated gold electrodes, the current density of outer-sphere electron transfer reactions, e.g. $Ce^{3+} \rightarrow Ce^{4+} + e^-$ decreases up to $d = 15$ Å according to Equation 14 but then the influence of d decreases, and finally i becomes independent of thickness since the ETR takes place via the conduction band of the oxide [80]. Similar results were obtained on passive iron [78]. In the case of

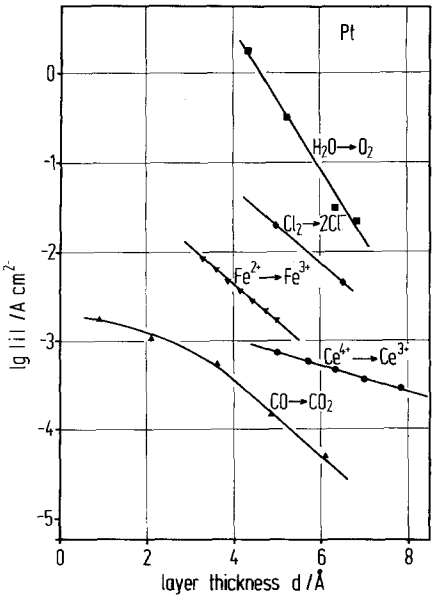

Fig. 7. Electronic influence of d_{PtO} on the rate of various ETR and CBR on Pt. $2H_2O \rightarrow O_2 + 4H^+ + 4e^-$ at 2·0 V [29], $Cl_2 + 2e^- \rightarrow 2Cl^-$ at 1·0 V [98], $Fe^{2+} \rightarrow Fe^{3+} + e^-$ [99], $Ce^{4+} + e^- \rightarrow Ce^{3+}$ at 0·95 V [28], and $CO + H_2O \rightarrow CO_2 + 2H^+ + 2e^-$ [27].

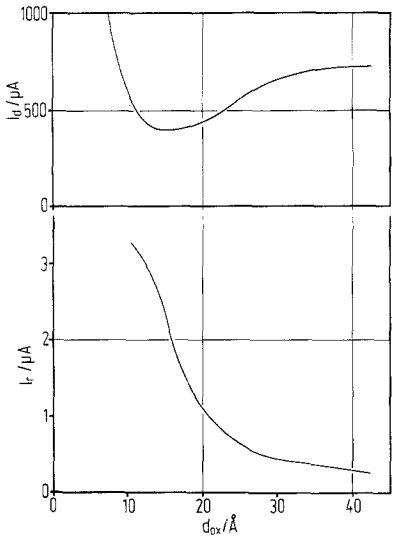

Fig. 8. Influence of d_{ox} of the sandwich oxide Au_2O_3 / $Au(OH)_3$ on ETR and CBR measured at the ring disc electrode in 1 N H_2SO_4 at 2·1 V [80]. I_r = ring current indicating the rate of $Ce^{3+} \rightarrow Ce^{4+} + e^-$ at the disc electrode (electronic influence on ETR). I_d = disc current due to oxygen evolution mainly (chemical influence on CBR for $d > 15$ Å).

passive titanium, anodic ETR are blocked totally [81]. The implantation of metal atoms into the oxide, e.g. Pt atoms, increases the electronic conductivity of the oxide, and electron transfer takes place by resonance tunnelling [81]. In principle, it should be possible to change the character of the semiconducting layer by doping from n- to p-type, which would allow a change from anodic to cathodic blocking. This, however, has not been done up till now.

Not all effects of oxide layers, however, are electronic effects. For example, parts a and b of Fig. 6 are due to chemical catalysis and geometric blocking. Further, the anodic oxygen evolution on gold oxide layers increases with increasing thickness after a minimum at about 15 Å, despite a further decrease in electronic conductivity of the oxide. This can be seen from Fig. 8 which refers to a simultaneous measurement of ETR and CBR on gold oxide by a ring disc electrode. (For details, see the caption of Fig. 8). The oxygen evolution is a CBR, and this depends sensitively on the surface composition of the oxide. In the case of gold oxide, a second layer of $Au(OH)_3$ grows at high potentials on an underlying layer of Au_2O_3. From the experimental results shown in Fig. 8, it must be concluded that this layer participates in the reaction and has a larger catalytic activity than the underlying gold oxide. Hence, the increase of rate is due to a chemical influence which overlaps the decrease of electronic conductivity which can be demonstrated by the ETR Ce^{3+}/Ce^{4+}. This effect can be shown even better with an indifferent oxide layer deposited on the first gold oxide. Very recently it was shown that oxygen evolution increases if a thin layer of FeOOH is deposited anodically on the gold oxide. Such a sandwich oxide has much better chemical properties than the gold oxide [82]. Photoelectrochemical effects on thin layers are of great importance since photoproduction of holes and electrons can induce electrode reactions such as hydrogen or oxygen evolution. These effects are strongly connected with the electronic properties of semiconducting layers. Further, electronic effects occur in adsorbed dye layers and increase the sensitivity to light absorption [90–96].

9. Conclusions

Electrocatalysis and inhibition by electrosorbates and protective layers is a three-parameter problem: it depends on

(a) the type of layer (ionic, covalent, neutral, oxide, salt),

(b) the type of reaction (ETR, ITR, CBR) and

(c) the type of influence (electrostatic, chemical, geometric, electronic).

Special models describe the various influences. Comparison with experiment shows qualitative and, in special systems, quantitative agreements which allow a general statement.

With ionic adsorbed layers, the main influence is electrostatic, but for some cases, these layers are found to have chemical influence too. Covalent layers may influence the rate of ITR and CBR by chemical interaction or by geometric blocking. Adsorbed neutral molecules and polymers cause a geometric blocking. For oxide and salt layers, the effect is geometric blocking at $\theta < 1$, a change of electronic interaction for thicker layers for all reactions and a chemical influence of the surface for ITR and CBR.

A formal analysis of experimental results with respect to θ and T is not so distinctive. For example, an exponential influence of θ can be explained by electrostatic interactions (Equations 8–10), by geometric blocking (Equations 11 and

12) and, with respect to thickness, by electronic effects (Equation 14). On solid surfaces, the influence of surface heterogeneity can cause further complications, since each crystal plane must be treated separately. Similarly, measurements of the temperature dependence are not conclusive. A change of activation energy may be explained by chemical effects, but the electrostatic interactions (Equations 9 and 10) and the geometric blocking (Equation 12) also cause changes in $\Delta H^{\ddagger}$. In Equations 8 and 11 a temperature dependence is not shown explicitly, but it is involved in B, the second virial coefficient.

In the case of multi-step reactions, the formal analysis is even more complicated, since a change of mechanism can be dominating or an inhibition of poisoning appears to be a catalysis. Hence, the detailed clarification of electrocatalysis and inhibition presumes a tedious analysis of the whole system, i.e. determination of surface structure, coverage and mechanisms and a complete determination of the parameters of Equation 3. Since experimental data are less complete in most cases, the explanation of catalysis and inhibition can be preliminary only.

Acknowledgements

The support of this work by the Deutsche Forschungsgemeinschaft is gratefully acknowledged. The authors are thankful to Dr F. D. Koppitz for helpful suggestions and discussions.

References

[1] H. Fischer, 'Elektrolytische Abscheidung und Elektrokristallisation von Metallen', Springer–Verlag, Berlin (1954).
[2] H. Fischer, *Werkstoffe und Korrosion* **6** (1972) 446, 452.
[3] H. Fischer, *Electrochim. Acta* **2** (1960) 50, 64.
[4] H. Fischer and H. Yamaoka, *ibid* **10** (1965) 679.
[5] H. Fischer, M. Knaack and O. Volk, *Z. Elektrochem.* **61** (1957) 123.
[6] H. Fischer and G. Thoresen, *ibid* **62** (1958) 235.
[7] H. Fischer, E. Schaaf and G. Thoresen, *ibid* **63** (1959) 427.
[8] H. Fischer, *Chem. Ing. Techn.* **36** (1964) 58.
[9] A. Frumkin, *Z. Phys. Chem.* **164** (1933) 121.
[10] R. Parsons, *J. Electroanalyt. Chem.* **21** (1969) 35.
[11] R. Parsons, *Ann. Univ. Ferrara Sez.* **5** (1970) Suppl. 5/3.
[12] W. Lorenz and W. Müller, *Z. Phys. Chem.* **18** (1958) 142.
[13] B. Kastening, *Ber. Bunsenges. Phys. Chem.* **68** (1964) 979.
[14] L. M. Peter, W. Dürr, P. Bindra and H. Gerischer, *J. Electroanalyt. Chem.* **71** (1976) 31.
[15] R. Guidelli and M. L. Foresti, *Electrochim. Acta* **18** (1973) 301.
[16] M. L. Foresti, D. Cozzi and R. Guidelli, *J. Electroanal. Chem.* **53** (1974) 235.
[17] T. Biegler and H. A. Laitinen, *J. Electrochem. Soc.* **113** (1966) 852.
[18] S. Sathyanarayana, *J. Electroanalyt. Chem.* **50** (1974) 195.
[19] J. Lipkowski and Z. Galus, *ibid* **61** (1975) 11.
[20] V. K. Venkatesan, B. B. Damaskin and N. N. Nikolaeva-Fedorovich, *Zh. Fiz. Khim* **39** (1965) 129.
[21] M. A. Loshkarev, F. I. Danilov and V. F. Voloshin, *Elektrokhimiya* **7** (1971) 868.
[22] L. A. Ternovskai, B. N. Afanasev and G. S. Ginsburg, *ibid* **8** (1972) 1119.
[23] R. R. Adzic and A. R. Despic, *Z. Phys. Chem.* **98** (1975) 95.
[24] R. R. Adzic, D. N. Simic, A. R. Despic and D. M. Drazic, *J. Electroanalyt. Chem.* **65** (1975) 587.
[25] H. Binder, A. Köhling and G. Sandstede, *Advan. Chem. Ser.* **90**, *Fuel Cell Systems II* (1969) 128.
[26] H. Binder and A. Köhling, 'From Electrocatalysis to Fuel Cells' (ed. G. Sandstede), Battelle Research Centre, Seattle (1972).
[27] C. H. Haman, *Ber. Bunsenges. Phys. Chem.* **75** (1971) 542.
[28] P. Kohl and J. W. Schultze, *ibid* **77** (1973) 953.
[29] J. W. Schultze and K. J. Vetter, *Electrochim. Acta* **18** (1973) 889.
[30] J. W. Schultze and M. Haga, *Z. Physik. Chemie NF* **104** (1977) 73.
[31] K. J. Vetter, 'Elektrochem. Kinetik', Springer–Verlag, Berlin (1961).
[32] W. Jaenicke and P. H. Schweitzer, *Z. Phys. Chem. NF* **52** (1967) 104.
[33] R. A. Marcus, *J. Chem. Phys.* **24** (1956) 996.
[34] *Idem, ibid* **26** (1957) 867.
[35] *Idem, ibid* **38** (1963) 1858.
[36] *Idem, ibid* **39** (1963) 1734.
[37] *Idem, Discuss. Farad. Soc.* **29** (1961) 21.
[38] *Idem, J. Phys. Chem.* **67** (1963) 853, 2889.
[39] R. W. Gurney, *Proc. Roy. Soc.* **134A** (1931) 137.
[40] H. Gerischer, *Z. Physik. Chem. NF* **26** (1960) 223, 325.
[41] M. J. Weaver and F. C. Anson, *J. Electroanalyt. Chem.* **65** (1975) 737.
[42] C. W. De Krenk, M. Sluyters-Rehbach and J. H. Sluyters, *ibid* **28** (1970) 391.
[43] J. W. Schultze and F. D. Koppitz, *Electrochim. Acta* **21** (1976) 326, 337.
[44] H. Wroblowa, Z. Kovac and J. O'M. Bockris, *Trans. Farad. Soc.* **61** (1965) 1523.
[45] M. Sluyters-Rehbach, J. S. M. C. Brenkel and J. H. Sluyters, *J. Electroanalyt. Chem.* **19** (1968) 85.
[46] D. Döhnert, J. Koutecký and J. W. Schultze, *ibid* **82** (1977) 81.
[47] J. C. Radacanu and W. J. Lorenz, *Electrochim. Acta* **16** (1971) 995.
[48] J. C. Radacanu and W. J. Lorenz, *ibid* **16** (1971)

1143.
[49] J. W. Schultze, *Proceedings of the 4th International Symposium on Passivity* Airlie, Virginia (1977).
[50] J. W. Schultze, *ISE Meeting*, Zurich (1976), Ext. Abstr. No. 116.
[51] A. A. El Miligy, D. Geana and W. J. Lorenz, *Electrochim. Acta* **20** (1975) 273.
[52] S. Schuldiner, *J. Electrochem. Soc.* **116** (1969) 767.
[53] H. H. Strehblow and J. Wenners, *Electrochim. Acta* **22** (1977) 421.
[54] A. N. Dey, *ibid* **21** (1976) 377.
[55] R. Parsons, in 'Advances in Electrochemistry and Electrochemical Engineering', Vol. 1, Intersciences New York (1961).
[56] P. Teppema, M. Rehbach Sluyters and J. H. Sluyters, *J. Electroanalyt. Chem.* **16** (1968) 165.
[57] E. Eriksrud, *ibid* **49** (1974) 77.
[58] R. Guidelli and M. L. Foresti, *ibid* **53** (1974) 219.
[59] *Idem, ibid* **67** (1976) 231.
[60] R. Guidelli and G. Pezzatini, *ibid* **76** (1977) 51, 61, 73.
[61] J. W. Schultze and K. J. Vetter, *ibid* **44** (1973) 63.
[62] *Idem, ibid* **53** (1974) 67.
[63] N. S. Hush, *J. Chem. Phys.* **28** (1958) 962.
[64] R. Guidelli, *J. Electroanalyt. Chem.* **53** (1974) 205.
[65] W. R. Fawcett and S. Levine, *ibid* **43** (1973) 175.
[66] S. Sathyanarayana, *ibid* **10** (1965) 119.
[67] M. S. Abdelal, A. A. Miligy, G. Reiners and W. J. Lorenz, *Electrochim. Acta* **20** (1975) 507.
[68] D. Dickertmann, J. W. Schultze and K. J. Vetter, *J. Electroanalyt. Chem.* **55** (1974) 429.
[69] F. G. Will, *J. Electrochem. Soc.* **112** (1965) 451.
[70] J. W. Schultze and D. Dickertmann, *Surface Sci.* **54** (1976) 489.
[71] N. Furuya and S. Motoo, *J. Electroanalyt. Chem.* **72** (1976) 165.
[72] R. R. Adzic and A. R. Despic, *J. Chem. Phys.* **61** (1974) 3482.
[73] H. W. Nürnberg, private communication (1967).
[74] M. J. Weaver and F. C. Anson, *J. Electroanalyt. Chem.* **65** (1975) 759.
[75] L. Pospisil and R. deLevie, *ibid* **25** (1970) 245.
[76] R. deLevie, *J. Electrochem. Soc.* **118** (1974) C 185.
[77] U. Stimming and J. W. Schultze, *Ber. Bunsenges. Phys. Chem.* **80** (1976) 1297.
[78] J. W. Schultze and U. Stimming, *Z. Phys. Chem. NF* **98** (1975) 285.
[79] W. Schmickler and J. W. Schultze, *ibid* (1978) in press.
[80] P. Kohl, dissertation, Freie Universität Berlin (1978).
[81] J. W. Schultze and U. Stimming, *ISE Meeting* Budapest, (1978). Extended Abstracts p. 409.
[82] J. W. Schultze, M. M. Lohrengel and P. Richter, *Ber. Bunsengs. Phys. Chem.* (1978) submitted.
[83] K. J. Vetter and J. W. Schultze, *ibid* **76** (1972) 920, 927.
[84] W. Lorenz, *Z. Phys. Chem. (Leipzig)* **218** (1961) 259, 272.
[85] *Idem, ibid* **219** (1962) 421.
[86] *Idem, ibid* **224** (1963) 145.
[87] *Idem, ibid* **227** (1964) 419.
[88] *Idem, ibid* **232** (1966) 176.
[89] W. Lorenz and G. Salie, *Z. Phys. Chem. NF* **29** (1961) 390, 408.
[90] K. L. Hardee and A. J. Bard, *J. Electrochem. Soc.* **123** (1976) 1024.
[91] H. Gerischer, *Farad. Disc. Chem. Soc.* **58** (1974) 219.
[92] H. Göhr and A. Breitenstein, *Electrochim. Acta* **13** (1968) 1377.
[93] G. Krüger, *ibid* **13** (1968) 1389.
[94] R. Memming, *Faraday Disc. Chem. Soc.* **58** (1974) 261.
[95] W. Paatsch, *Ber. Bunsenges. Physik. Chem.* **79** (1975) 922.
[96] W. J. Wesselowski, *Elektrokhimyia* **9** (1973) 1557.
[97] Z. A. Jofa, B. Kabanov, E. Kuchinskii and F. Chistyakov, *Acta Physicochim. USSR* **10** (1939) 317.
[98] T. Dickinson, R. Greef and L. Wynne-Jones, *Electrochim. Acta* **14** (1969) 467.
[99] D. H. Angel and T. Dickinson, Extended Abstracts, *CITCE Meeting*, Prague (1970) p. 111.
[100] M. W. Breiter, *J. Electroanalyt. Chem.* **65** (1975) 623.
[101] T. Erdey-Gruz, 'Kinetics of Electrode Processes', Adam Hilger Ltd, London (1972).
[102] K. J. Vetter and J. W. Schultze, *J. Electrochem. Soc.* **116** (1969) 824.
[103] H. Gerischer, Nat. Bur. Stand. Publication 455 (November 1976).
[104] D. G. Wierse, M. M. Lohrengel and J. W. Schultz, *J. Electroanalyt. Chem.* **92** (1978) 121.